Supporting information:

Structure-dependent luminescence of Eu^{3+}-doped strontium vanadates, synthesized at different V:Sr ratios – application for WLED and ultra-sensitive optical thermometry

Przemysław Woźny[a], Kevin Soler-Carracedo[b], Natalia Stopikowska[a], Inocencio R. Martin[b] , Marcin Runowski[a.b]*

[a]Adam Mickiewicz University, Faculty of Chemistry, Uniwersytetu Poznańskiego 8, 61-614 Poznań, Poland

[b]Universidad de La Laguna, MALTA-Consolider Team, IMN and IUdEA, Departamento de Física, Apdo. Correos 456, E-38200, San Cristóbal de La Laguna, Santa Cruz de Tenerife, Spain

Corresponding Authors

P.W.: przemyslaw.wozny@amu.edu.pl

Solutions preparation for synthesis:

The $Sr(NO_3)_2$ (Sigma-Aldrich, ACS >99%) was dissolved in deionized water to form a solution (0.5 M). The starting material Eu_2O_3 (Stanford Materials, 99.99%) was dissolved in excess of the HNO_3 (67%, PoCH, pure, p.a.), next deionized water was added and evaporated three times to remove HNO_3 residues. In the end, the $Eu(NO_3)_3$ was dissolved in deionized water to prepare a solution (0.5 M).

Structural analysis:

In the main manuscript, only selected diffractograms for the obtained structure were presented. In research, more materials around 0.67 V:Sr ratio was prepared to synthesize pure crystal structure. Here, we present diffractograms for all prepared materials in a full range of V:Sr ratio used in synthesis. We choose the material with 0.67 V:Sr for further analysis.

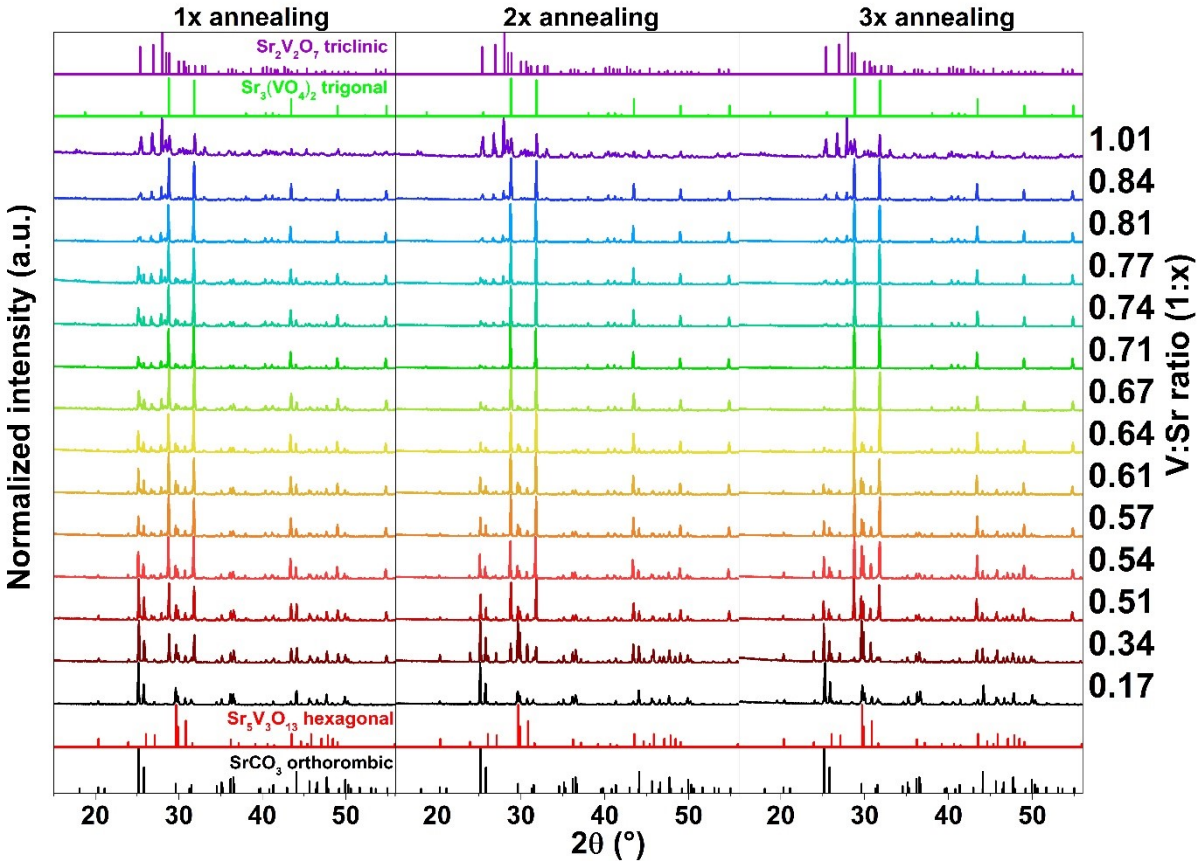

Figure S1. The X-ray diffraction patterns for all materials obtained with alternated V:Sr ratio.

Based on SEM images presented in **Figure 3b** size of the crystals grains were measured using ImageJ software. Obtained values of particle number and size of grains allow preparing a histogram of size distribution. The mean size of particles was calculated as 0.998 μm, but the high value of standard deviation (0.433 μm) is evidence of broad particle size distribution.

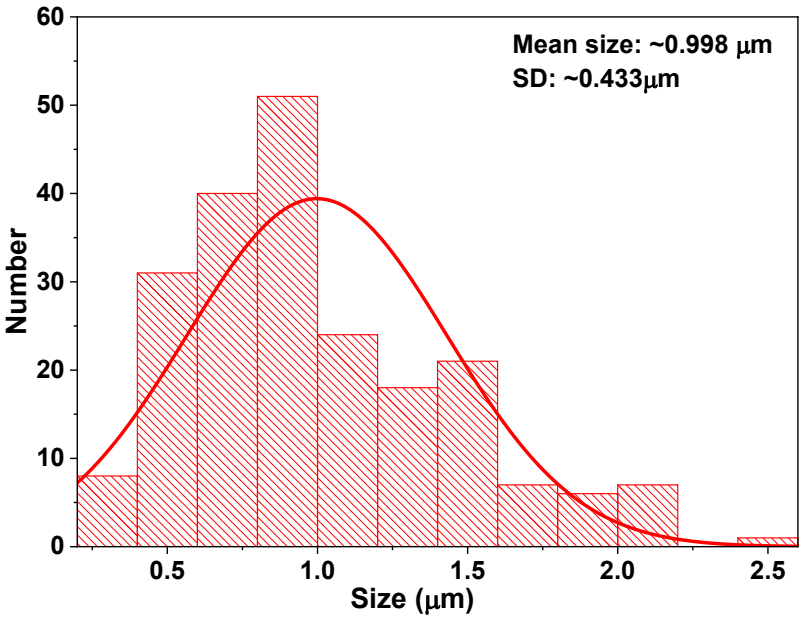

Figure S2. Histogram of the grain size for $Sr_3V_2O_8$: Eu^{3+} material obtained with 0.67 V:Sr ratio.

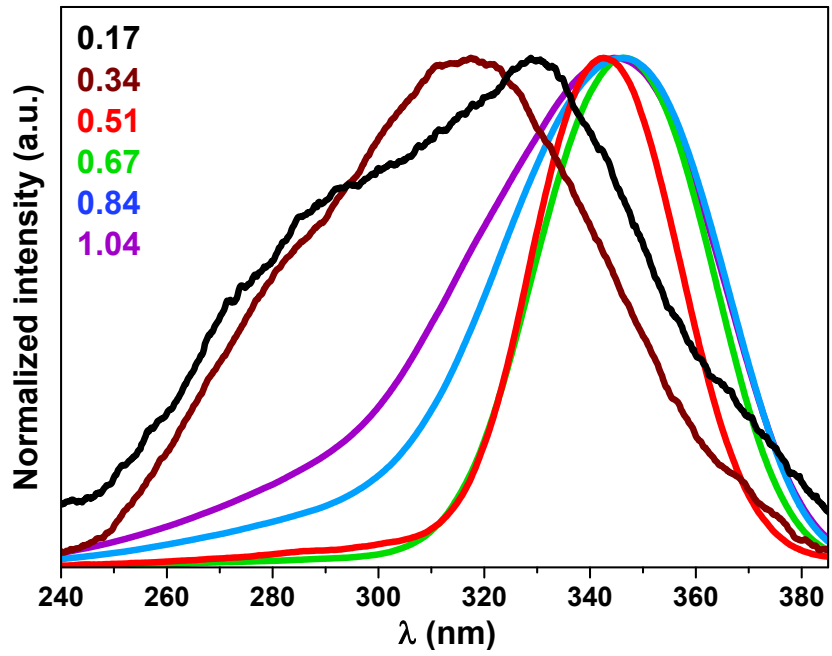

Figure S3. Normalized excitation spectra for λ_{em} at 540 nm for materials with different V:Sr ratios.

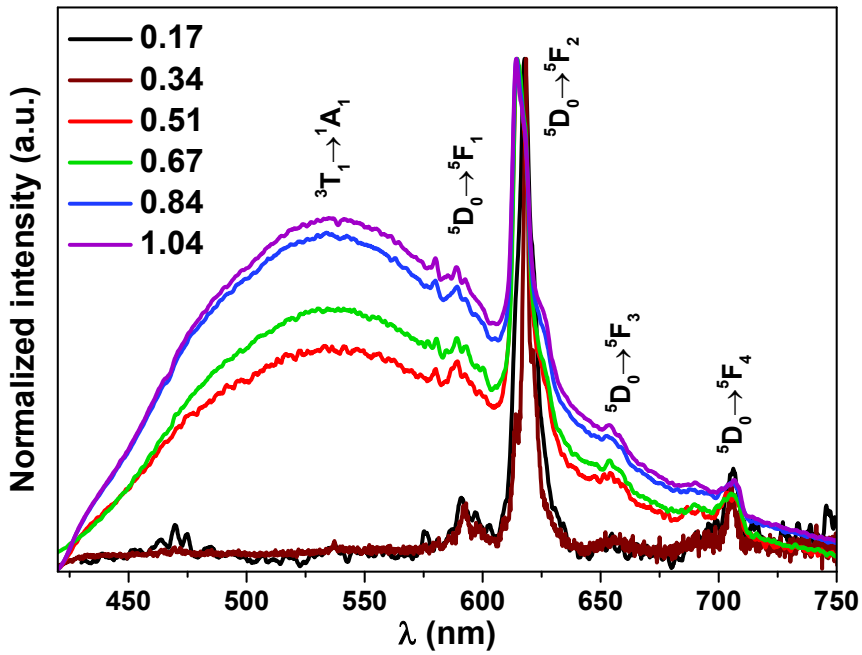

Figure S4. Normalized emission spectra recorded at λ_{ex} = 345 nm for materials with different V:Sr ratios.

The shape of the Eu^{3+} ions emission bands is changed according to changes in the crystal structure. Material with the lowest V:Sr ratio (0.17) presents broad, overlapped sublevels with the maximum at λ = 614 nm for the $^5D_0 \rightarrow {}^7F_2$ transition. Next, the maximum emission was shifted to λ = 615 nm where the hexagonal structure dominates. In materials with trigonal $Sr_3V_2O_8$ crystal structure decrease of the band at λ=615 nm occurred, and the maximum emission was observed at λ = 612 nm. Increase of the V:Sr ratio and the presence of $Sr_2V_2O_7$ crystal

structure caused the band's separation at 612 nm for two bands at λ = 611 and 613 nm. Other differences were seen for the $^5D_0 \rightarrow {}^7F_0$ transition, where the low V:Sr ratio (0.17, 0.34) band with a maximum at λ = 573 nm was observed, for materials with higher V:Sr (0.51,0.67,0.84) the maximum was recorded at λ = 577 nm. An increase of vanadium species used in the synthesis caused changes in crystal structure and observation of split bands at λ = 578 nm.

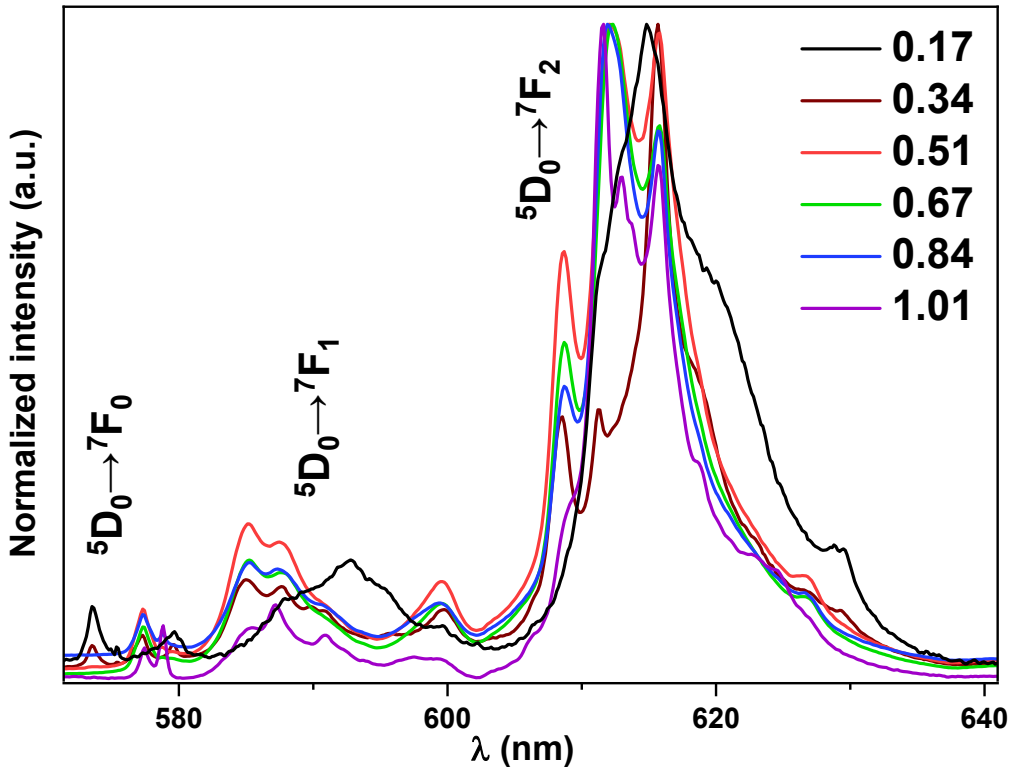

Figure S5. Normalized emission spectra recorded at λ_{ex} = 393 nm for materials with different V:Sr ratios.

The normalized emission spectra of the $Sr_3V_2O_8$ doped with altered Eu^{3+} ion concentration show minor changes in the hypersensitive $^5D_0 \rightarrow {}^7F_2$ transition band. With an increase of Eu^{3+} ions content above 2% two additional Stark sub-levels, i.e., at λ = 614 nm and λ = 618 nm start to appear, probably due to starting of incorporation into another site of Sr^{2+} ions in the crystals structure.

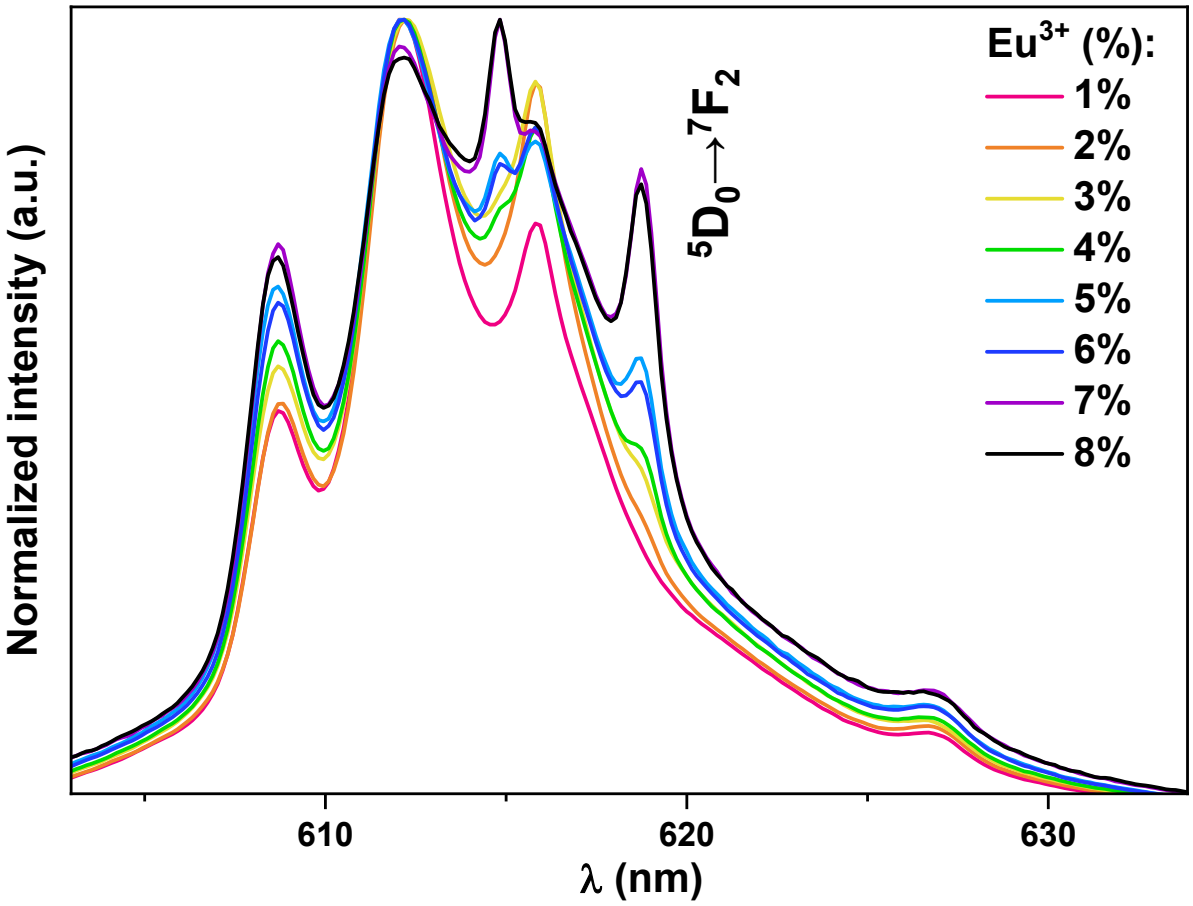

Figure S6. Normalized emission spectra recorded at λ_{ex} = 393 nm for $Sr_3V_2O_8$ materials with different Eu^{3+} ions content.

Asymmetry parameters increased from 1% to 2% of Eu^{3+} ions content, and decreases with further Eu^{3+} ions content incensement (**Figure S7**). Obtained results are evidence of increasing symmetry of the Eu^{3+} ions surrounding above 2% of Eu^{3+} ions content.

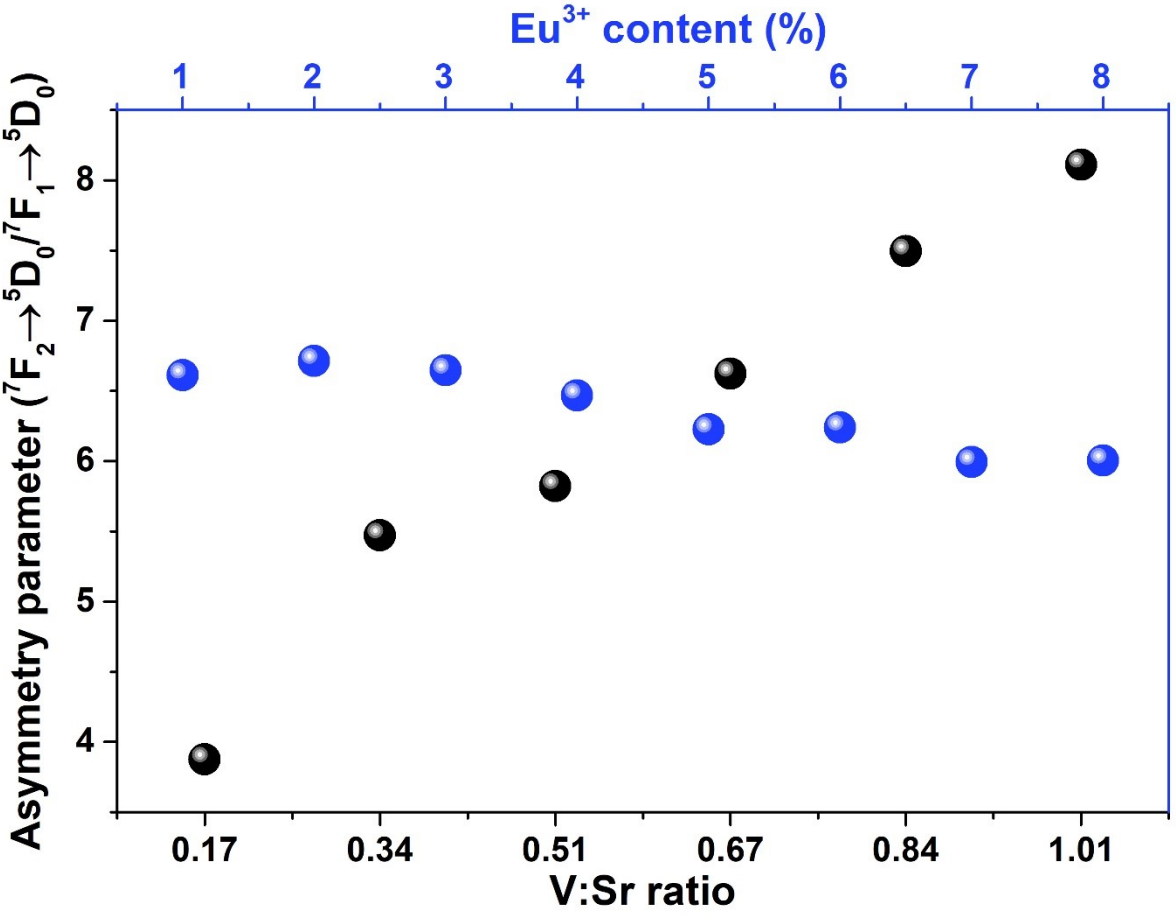

Figure S7. Asymmetry parameter ratio for the materials synthesized with alterated V:Sr ratio and altered Eu^{3+} ions content.

Table S1. Asymmetry parameter, total radiative transition probabilities (A_{Tot}), radiative transition probabilities for each transition ($A_{5D0\rightarrow7FJ}$), and intensity parameters (Ω_2 and Ω_4) for materials obtained with changed V:Sr ratio.

V:Sr	Asymm. Par.	A_{Tot} (s^{-1})	$A_{5D0\rightarrow7F1}$ (s^{-1})	$A_{5D0\rightarrow7F2}$ (s^{-1})	$A_{5D0\rightarrow7F4}$ (s^{-1})	Ω_2 (10^{-20} cm^2)	Ω_4 (10^{-20} cm^2)
0.17	3.877	1226.742	116.272	880.440	230.031	11.204	6.084
0.34	5.473	1094.324	116.827	780.884	196.613	9.872	5.167
0.51	5.823	1115.767	117.027	787.258	211.482	9.888	5.536
0.67	6.623	1170.958	116.996	837.023	216.939	10.512	5.683
0.84	7.495	1255.365	117.060	904.538	233.768	11.342	6.125
1.01	8.112	1713.122	117.386	1303.867	291.870	16.416	7.659

Table S2. Asymmetry parameter, total radiative transition probabilities (A_{Tot}), radiative transition probabilities for each transition ($A_{5D0\rightarrow 7FJ}$), and intensity parameters (Ω_2 and Ω_4) for materials obtained with different Eu^{3+} ions concentration.

Eu^{3+} (%)	Asymm. Par.	A_{Tot} (s^{-1})	$A_{5D0\rightarrow 7F1}$ (s^{-1})	$A_{5D0\rightarrow 7F2}$ (s^{-1})	$A_{5D0\rightarrow 7F4}$ (s^{-1})	Ω_2 (10^{-20} cm^2)	Ω_4 (10^{-20} cm^2)
1	6.611	1104.788	116.984	773.337	214.467	9.709	5.612
2	6.715	1116.669	116.966	785.474	214.229	9.867	5.607
3	6.647	1111.945	116.940	777.354	217.650	9.766	5.695
4	6.468	1091.233	116.981	756.681	217.571	9.506	5.692
5	6.226	1060.502	116.980	728.349	215.173	9.152	5.628
6	6.241	1060.987	116.999	730.208	213.780	9.176	5.593
7	5.995	1030.192	116.970	701.281	211.942	8.823	5.547
8	6.005	1028.304	116.933	702.153	209.218	8.834	5.475

Figure 12a, b present changes of the LIR parameter and band centroid shift of the overlapped CTB and Eu^{3+} ions emission, respectively. Experimental data points were fitted ($R^2 \approx 0.99$) using the fifth-order polynomial functions below:

$$LIR = A_0 + A_1T^1 + A_2T^2 + A_3T^3 + A_4T^4 + A_5T^5$$

Here, A_0, A_1, A_2, A_3, A_4 and A_5 are constants and T is temperature. Herein, these constants are fitted to be A_0 = -35.58, A_1 = 0.43, A_2 = -1.94*10-3, A_3 = 4.30*10-6, A_4 = -4.69*10-9, and A_5 = 2.03*10-12.

The temperature-dependent can be fitted by using other fifth-order polynomial:

$$Centroid = A_0 + A_1T^1 + A_2T^2 + A_3T^3 + A_4T^4 + A_5T^5$$

Herein, these constants A_0-A_5 are fitted to be A_0 = 1122.71, A_1 = -6.24, A_2 = 0.03, A_3 = -6.02*10-5, A_4 = 6.50*10-8 and A_5 = -2.85*10-11.

Figure S8 present calculated integrated intensities (area under the spectra) for both CTB ($\lambda \approx 453 – 566$ nm) and Eu^{3+} ion ($\lambda \approx 568 – 631$ nm) emission after excitation at λ_{ex} = 375 nm as a function of temperature. Because the CTB and Eu^{3+} ion emission spectra overlap, the CTB contributions (in the range of Eu^{3+} emission) were used as a baseline to obtain the integrated intensities of the Eu^{3+} ions. It needs to be mentioned that those values were used to further LIR calculation.

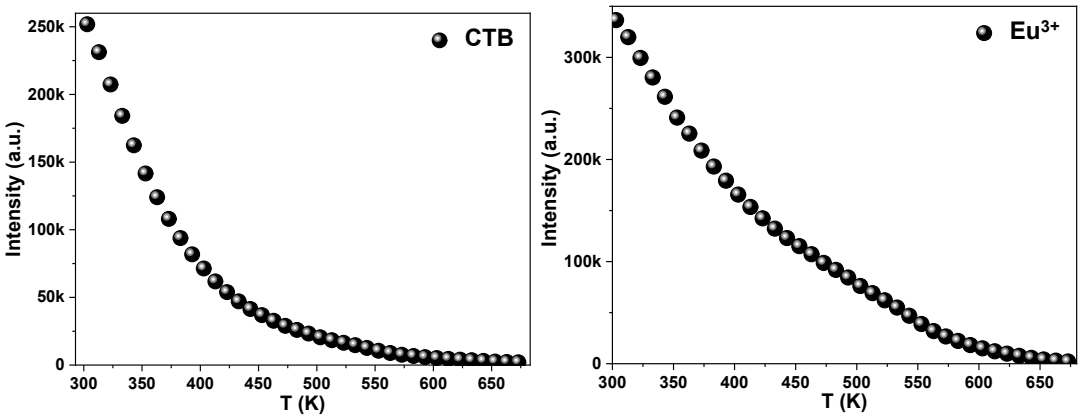

Figure S8. Intensity emission changes for two components in the function of temperature.